NANO MICRO small

Supporting Information

for *Small*, DOI: 10.1002/smll.201701763

Controlling Plasmon-Enhanced Fluorescence via Intersystem Crossing in Photoswitchable Molecules

*Mingsong Wang, Gregory Hartmann, Zilong Wu, Leonardo Scarabelli, Bharath Bangalore Rajeeva, Jeremy W. Jarrett, Evan P. Perillo, Andrew K. Dunn, Luis M. Liz-Marzán, Gyeong S. Hwang, and Yuebing Zheng**

Supporting Information

Controlling Plasmon-Enhanced Fluorescence via Intersystem Crossing in Photoswitchable Molecules

*Mingsong Wang, Gregory Hartmann, Zilong Wu, Leonardo Scarabelli, Bharath Bangalore Rajeeva, Jeremy W. Jarrett, Evan P. Perillo, Andrew K. Dunn, Luis M. Liz-Marzán, Gyeong S. Hwang, Yuebing Zheng**

M. Wang, Z. Wu, B. Bangalore Rajeeva, Prof. Dr. Y. Zheng
Department of Mechanical Engineering
Texas Materials Institute
The University of Texas at Austin
Austin, TX 78712, USA
E-mail: zheng@austin.utexas.edu (Y. B. Z.)
G. Hartmann, Prof. Dr. G. S. Hwang
Department of Chemical Engineering
The University of Texas at Austin
Austin, TX 78712, USA
Dr. L. Scarabelli, Prof. Dr. L. M. Liz-Marzán
Bionanoplasmonics Laboratory
CIC biomaGUNE
Paseo de Miramón 182, 20014 Donostia-San Sebastián, Spain
Dr. L. Scarabell
Department of Chemistry and Biochemistry,
California NanoSystems Institute,
University of California, Los Angeles,
Los Angeles, California 90095, USA
Prof. Dr. L. M. Liz-Marzán
Ikerbasque, Basque Foundation for Science
48013 Bilbao, Spain
Prof. Dr. L. M. Liz-Marzán
Biomedical Research Networking Center in Bioengineering, Biomaterials, and Nanomedicine
CIBER-BBN, 20014 Donostia- San Sebastián, Spain
Dr. J. W. Jarrett, E. P. Perillo, Prof. Dr. A. K. Dunn
Department of Biomedical Engineering,
The University of Texas at Austin
Austin, TX 78712, USA

1. Fourier transform infrared (FTIR) and UV-vis absorption spectra

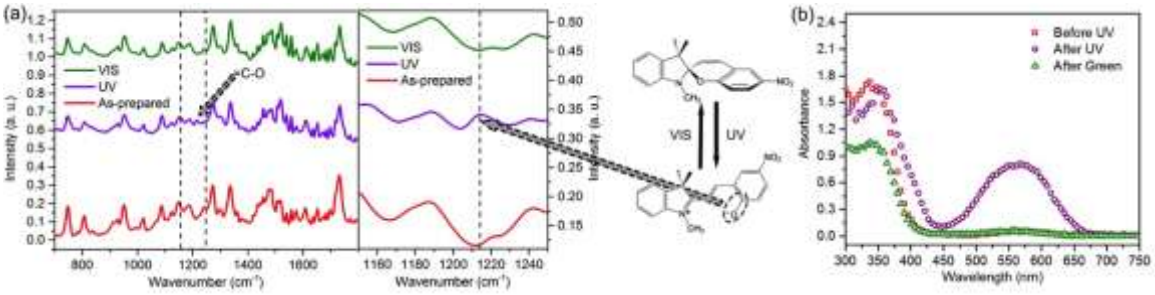

Figure S1. a) FTIR spectra of molecules under different light irradiation. The right panel is zoom-in spectra for the part indicated by dashed lines in the left panel. The dashed line in right panel indicates additional peak at 1214 cm^{-1}. The chemical structures of the molecules under isomerization are shown. b) UV-vis absorption spectra of molecules under different light irradiation.

FTIR spectra, shown in **Figure S1**, were used to characterize the molecular structures in the as-prepared sample, after UV irradiation and after visible light irradiation. After UV irradiation, an additional peak appears at 1214 cm^{-1} position, which is derived from =C-O band as shown in the chemical structure. This peak vanishes after visible light irradiation. From the schematics of molecular structures in **Figure 1**a and Figure S1a, it is known that =C-O band only appears after the ring-open process. Therefore, the appearance and disappearance of =C-O band in the FTIR spectra reveal that molecules were in the close form (SP form) in the as-prepared sample and changed to the open form (MC form) after UV irradiation. The FTIR spectra are consistent with the absorption spectra (Figure S1b) and previously reported results.[1-2]

2. Optical spectrum of the halogen light source

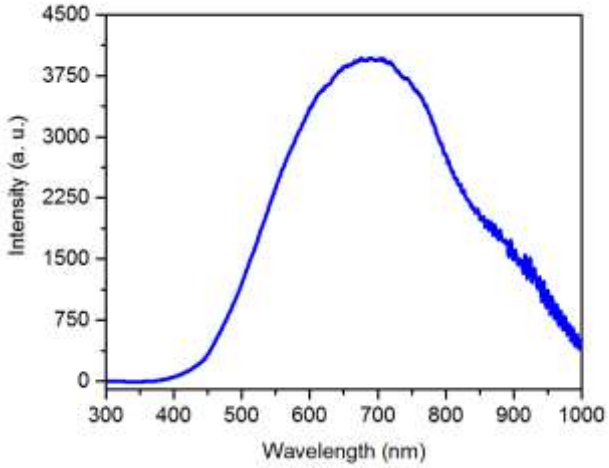

Figure S2. Optical spectrum of the halogen light source. The supply voltage of the light source is 6V.

3. Explanation of white-light-excited red fluorescence in as-prepared sample and the sample after green light irradiation

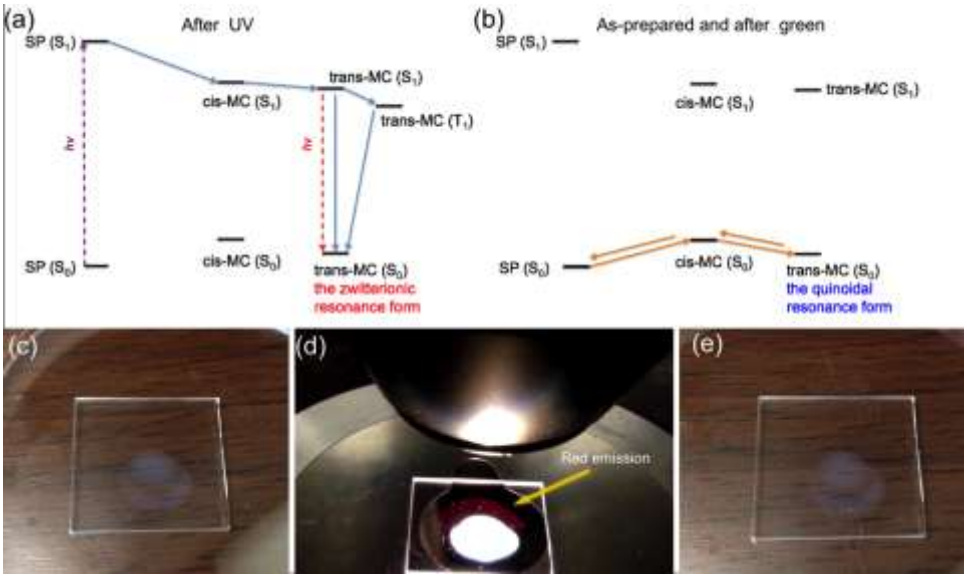

Figure S3. a) Schematic of the photochemical pathway.. b) Schematic of the thermal pathway. c) Photo of SP-doped PMMA film before white light irradiation. d) Red fluorescence from the SP-doped PMMA film immediately after white light irradiation. e) Photo of SP-doped PMMA film after 1 minute of white light irradiation.

To elucidate the origin of the red emission present in the as-prepared prepared sample and after green light irradiation, we consider the thermal ring-open process, which can be excited by the photothermal effect brought by the white light irradiation. Unlike the

photochemical ring-open process (**Figure S3**a), the thermal ring-open process allows the SP-MC isomerization to occur at ground states.[3] This leads to the transfer of SP molecules to MC molecules in the quinoidal resonance form (Figure S3b). Therefore, the fluorescence of quinoidal MC molecules is the origin of the red emission in the as-prepared sample and after green light irradiation. In addition, previous studies indicate that at ground state the activation energy of the ring-close process is lower than that of the ring-open process.[3] This low activation energy destabilizes MC molecules in a nonpolar environment (e.g. in the PMMA matrix) in room temperature, and allows MC to switch back to SP by a slight temperature increase, as shown in Figure S3b. But the ring-open process is a steric molecular change, which is much slower than the radiative decay, i.e., the fluorescence; therefore, MC molecules can emit photons before switching back to SP molecules. This manifests as an obvious red fluorescence under white light irradiation (comparing Figure S3c and Figure S3d), while the sample did not show the purple color that is caused by the absorption of MC molecules, after the white light irradiation (Figure S3e).

4. SEM and TEM images of AuNSs and AuNTs

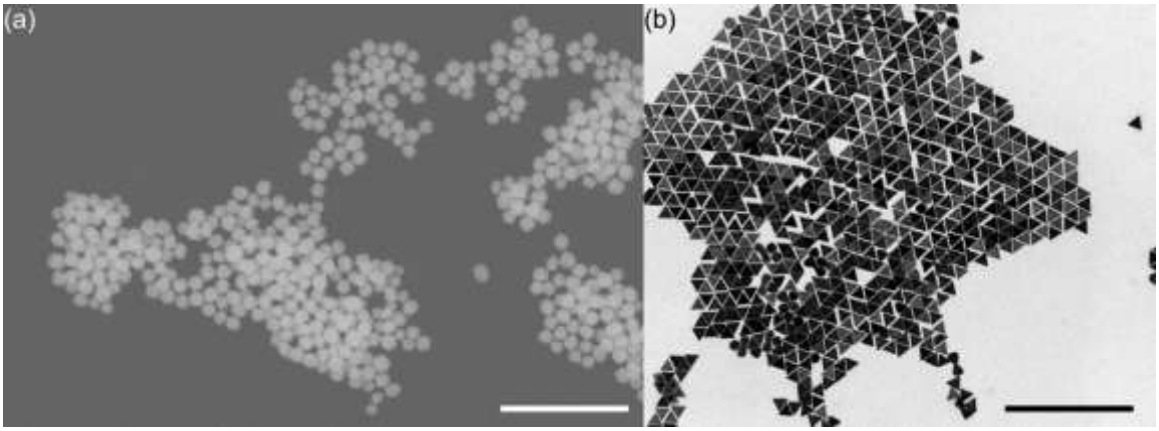

Figure S4. a) SEM image of AuNSs. Scale bar is 500 nm. b) TEM image of AuNTs. Scale bar is 500 nm.

5. Optical scattering spectra of single AuNTs

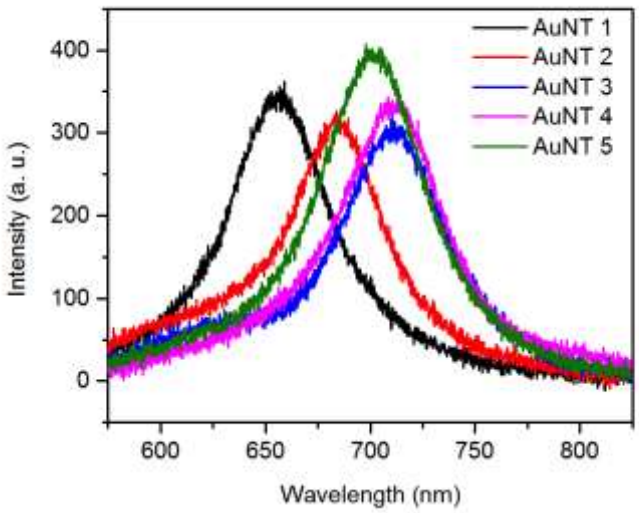

Figure S5. Optical scattering spectra of 5 single AuNTs coverd by PMMA.

6. Density Functional Theory (DFT) calculations of *trans*-MC structure and properties

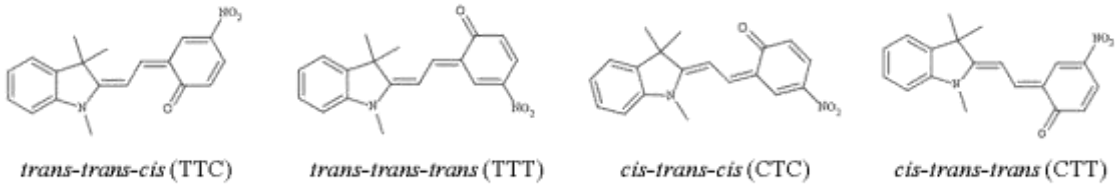

Figure S6. Skeletal formula of four *trans*-MC isomers.

Table S1. Predicted relative stabilities (ΔE), HOMO-LUMO gaps ($\Delta E_{HOMO\text{-}LUMO}$), and maximum absorption wavelengths (λ_{max}) of four *trans*-MC isomers shown above from implicit solvent DFT calculations using the B3LYP hybrid functional. Values in parenthesis were obtained using the PBE functional. The nomenclature applied represents the configuration of the stereocenters, ordered from the indoline group to the nitrobenzene group. Here, we assume that the dielectric constant (ε) of the PMMA matrix is 4.

	ΔE (eV)	$\Delta E_{HOMO\text{-}LUMO}$ (eV)	λ_{max} (nm)
TTC	0.00 (0.00)	2.76 (1.63)	505 (573)
TTT	0.05 (0.05)	2.66 (1.59)	530 (595)
CTC	0.08 (0.08)	2.76 (1.63)	506 (574)
CTT	0.11 (0.11)	2.67 (1.54)	529 (595)

Table S2. Predicted bond lengths (in Å) of the indicated C-C and C-O bonds in the gas phase (ε = 1) and in solvent (ε = 4) from implicit solvent DFT calculations using the B3LYP (PBE) functional.

	ε = 1	ε = 4
$d_{C\text{-}C}$	1.398(1.401)	1.387(1.393)
$d_{C\text{-}O}$	1.238(1.251)	1.244(1.255)

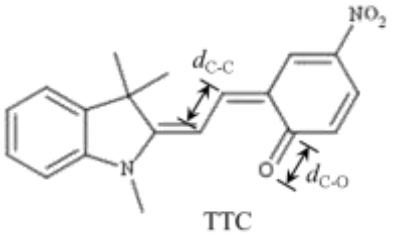

Table S3. Predicted HOMO-LUMO gap ($\Delta E_{HOMO-LUMO}$) and maximum absorption wavelength (λ_{max}) of the most stable *trans*-MC isomer (TTC) for variation of the dielectric constant (ε) of solvent from implicit solvent DFT calculations using the B3LYP (PBE) functional.

ε	$\Delta E_{HOMO-LUMO}$ (eV)	λ_{max} (nm)
2	2.72 (1.60)	510 (578)
4	2.76 (1.63)	505 (573)
6.32	2.77 (1.64)	502 (570)
78.4	2.82 (1.68)	495 (563)

The *trans*-MC stereoisomers (distinguished by the *trans* configuration of the central bond) were compared as described in **Table S1**. The ε of the monomer unit, methyl methacrylate, varies in the literature thus values within the range of 2-6.32 were compared (Table S3). We chose to represent the PMMA matrix using a dielectric constant of 4, within the center of the range of reported values for PMMA and the MMA monomer. Within this range of the dielectric constant, the wavelength of the first vertical excitation varies by less than 10 nm (see Table S3), meaning the intermediate value is accurate enough for comparison with the experimentally measured values. The stability difference between these stereoisomers is small enough to allow isomerization. Sheng *et al*. predicted using DFT that the activation energy barriers for the conversion between MC stereoisomers are on the order of 1 eV.[3] Confinement in the PMMA matrix may hinder the rotation of the molecule around the aliphatic bonds, increasing the isomerization barriers and MC in various stereoisomers. The less stable isomers have smaller gaps between the higher occupied molecular orbital (HOMO) and the lowest unoccupied molecular orbital (LUMO), as the torsion of the alkane bonds make them less stable. Vertical excitation calculations using TD-DFT predict a corresponding red shift of the first excited state in the isomers with smaller HOMO-LUMO gaps, as the first excited state is predicted to simply be the excitation from the HOMO to the LUMO.

7. Scattering spectra and SEM images of single 60 nm AuNSs

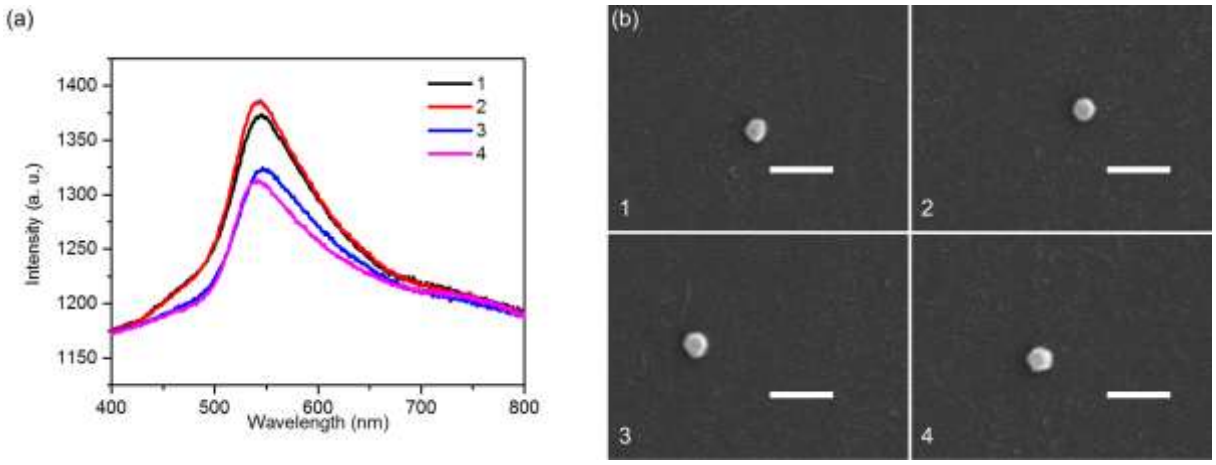

Figure S7. a) Scattering spectra of 4 single 60 nm AuNSs. b) SEM image of single 60 nm AuNSs of a). Scale bar is 200 nm.

References:

[1] R. Klajn, *Chem. Soc. Rev.* **2014**, 43, 148.
[2] Y. B. Zheng, B. Kiraly, S. Cheunkar, T. J. Huang, P. S. Weiss, *Nano Lett.* **2011**, 11, 2061.
[3] Y. Sheng, J. Leszczynski, A. A. Garcia, R. Rosario, D. Gust, J. Springer, *J.Phys. Chem. B* **2004**, 108, 16233.